USE OF THE ARTIFICIAL NEURAL NETWORK FOR PEAK GROUND ACCELERATION ESTIMATION

Boumédiène Derras[1,2] and Abdelmalek Bekkouche[2]
[1]Laboratoire de Géophysique Interne et Tectonophysique (LGIT), B.P. 53 – 38041, Université Joseph Fourier, CNRS, LCPC, Grenoble, France
[2]Laboratoire RISAM, Département de Génie Civil, Faculté de Technologie, Université AbouBekr Belkaid, Tlemcen, B.P. 230 Chetouane, Tlemcen 13000, Algérie
derrasb@obs.ujf-grenoble.fr

ABSTRACT

The aim of this paper is to estimate the maximum Peak Ground Acceleration (PGA) of the three components (vertical, east-west and north-south) using the feed-forward artificial neural network method (ANN) with a conjugate gradient backpropagation rule for the training. The inputs are the magnitude, the focal depth, the epicentral distance, the thickness of the sedimentary layers below the site down to a shear wave velocity equal to 800 m/s and the corresponding resonant frequency, while the target result is the PGA. Data collected from the KiK-net seismic data base in Japan have been used. 1850 records at 102 sites are considered in the training phase, while 326 records are kept for the test phase. The obtained results show that PGA computed using the ANN method are close to those recorded. Finally, a simple example is presented in which 55 records are used to compare the ANN method with two Ground Motion Prediction Equations (GMPEs). This example demonstrates how the ANN works and shows its potential.

INTRODUCTION

An important parameter for assessing the earthquake effects at a given location is the Peak Ground Acceleration (PGA). The importance of this parameter is revealed in the development of seismic zoning maps and the construction of design response spectra used in earthquake-resistant construction rules. The question is how to estimate PGA at a site where no accelerometric recording station is installed.

In order to predict PGA at a site, one usually relies on empirical GMPEs. These equations relate PGA to earthquake and site parameters. The development of such equations requires large database of recorded PGAs and associated metadata on earthquakes and sites (Ambraseys & Douglas, 2003; Takahashi *et al*., 2000; Lussou *et al*., 2001). These Ground Motion Prediction Equations (GMPEs) reflect the combination of three effects (source, path and site) using a physical model.

A functional form is given *a priori* based on the comprehension of the mechanisms that influence the surface signal. Douglas (2003) conducted an analysis on the Ground-Motion Prediction Equations developed in the last 30 years and found that each equation was developed using a variety of input parameters depending on available data which varies greatly with geographical regions. These authors also show that the functional forms vary very much as well.

To obtain a relationship Ground Motion Prediction Equation for PGA in a simple and easy way using a large amount of available seismic data, a new approach, based on artificial neural networks (ANN), is proposed in this paper. This method does not require *a priori* functional form.

This tool has proved its efficiency in solving complex nonlinear problems. The ANN has received, in recent years, a growing interest by the scientific community in the field of earthquake engineering and seismic risk assessment: site effect assessment in 1-D (Giacinto *et al*., 1997), or 2-D (Paolucci *et al*., 2000); generation of time histories compatible with target response spectrum (Ghaboussi & Lin, 1998; Chu-Chieh & Jamshid, 2001); estimation of artificial time history and related spectral response (Seung & Sang, 2002; Derras *et al*., 2010); and evaluation of liquefaction potential (Goh, 1994). In the same context, a neural model was developed by Baziar and Gharbani (2005) to predict the horizontal displacement due to soil liquefaction. Prediction of aftershocks from the main shock using a Bayesian neural network was also carried out by Vincenzo *et al.* (2006). Also, three other works were done. The first by Alves (2006) for the generation of the time history, the second for evaluation of the peak ground velocity (PGV) in the western region of the United States (Ben-yu *et al*., 2006), and the third by Irshad *et al.* (2008) on the evaluation of strong motion peak in Europe.

Regarding the estimation of PGA by ANN method, two recent studies were conducted by Tienfuan and King (2005) and Kemal and Ayen (2008). In the first article, the authors have used earthquake magnitude and focal depth, as well as epicentral source-to-site distances, as inputs for the ANN method, to estimate PGA. They used a limited network for ten stations deployed along the train tracks in Taiwan. The second article was focused on PGA prediction in the northwest region of Turkey. The authors used earthquake moment magnitude, hypocentral distance, focal depth, and site conditions as inputs. Three different artificial neural networks are used by Kemal and Ayen (2008) for PGA prediction, namely, feed-forward back-propagation (FFBP), Radial Basis Function (RBF), and Generalized Regression Neural Networks (GRNNs). Testing of result indicated that the FFBP gives the best estimation compared to GRNN and RBF.

An artificial neuron is a simple mathematical operator. This neuron receives one or more inputs and sums them to produce an output. Usually the sum of each node is weighted by coefficients (known as weights of connections or synaptic weights), and the sum is passed through a non-linear function known as an activation function. These functions usually have a sigmoid shape. They are also often monotonically increasing, continuous, differentiable and bounded. The activation function used in this article is Tanh-sigmoid function: $f(x) = \text{Tanh}(x)$. This choice was made after several tests.

The feed-forward back-propagation (FFBP) has a quite particular structure in which neurons are organized in successive layers (Figure 1). The first layer is called input layer, the

last layer is called output layer, and all intermediate layers are called hidden layers. Each neuron in a hidden layer receives signals from the previous layer net and transmits the result to the next layer *O*.

The operations of each jth neuron are described by the following two equations:

$$net_j = \sum_{i=1}^{N} w_{ij} \times x_i \quad 1 \leq j \leq N_h \tag{1}$$

And the output for the same neuron is expressed by: $O_j = f(net_j)$

w_{ij} being the connection weights between the ith neuron of the previous layer and the jth neuron of the current layer and *f* is the activation function.
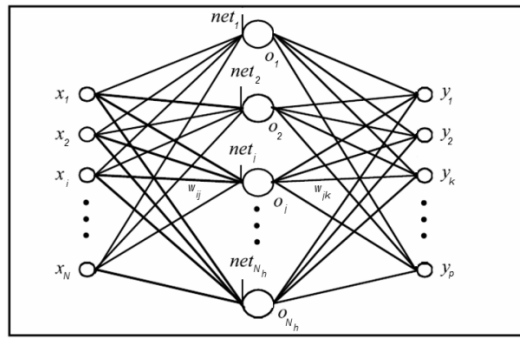

Figure 1. Feed-forward back-propagation (FFBP) (Yu *et al.*, 2002).

The training used for the FFBP neural network is supervised. The training data consist of many pairs of input/output training patterns. The algorithm used for this case is known as conjugate gradient backpropagation. This algorithm is almost as fast as the LM algorithm (Moré, 1978) on function approximation problems (faster for large networks). Its performance does not degrade when the error is reduced. The conjugate gradient algorithms have relatively modest memory requirements (Demuth *et al.*, 2009).

The back-propagation training method is divided into two stages (Coulibaly, 1999): propagation phase to present a configuration entry to the network and then propagate this entry from the input layer to the output layer through the hidden layers; and a back-propagation phase, to minimize the error on all the examples. This represents the mean squared error (*MSE*). It is the difference between desired and calculated responses for all data in the training set, or simply the difference between the desired outputs and those calculated by the ANN, defined by eq. (2).

$$MSE = \frac{\sum_{k=1}^{P} \sum_{l=1}^{E} (d_{kl} - y_{kl})^2}{N.P} \tag{2}$$

Where *E* is the data number, *P* is the number of neurons in the output layer (here *P*=1), d_{kl} is the desired output (in this case recorded PGA) for output neuron *k* and l^{th} data. y_{kl} is the output estimated (in this case model prediction of PGA) for output neuron k^{th} (here *k*=1) and l^{th} data. The *MSE* can be used to determine how well the network outputs fit the data.

In addition, the correlation coefficeint (R) was used. It indicates the degree of linear dependence between variables. In this study, the PGA are the variables recorded and those produced by the ANN by definition, the correlation coefficient between a network output y_l and a desired output d_l is ($k=p=1$):

$$R = \frac{\dfrac{\sum_l (y_l - \overline{y})(d_l - \overline{d})}{N}}{\sqrt{\dfrac{\sum_l (d_l - \overline{d})^2}{N}} \cdot \sqrt{\dfrac{\sum_l (y_l - \overline{y})^2}{N}}} \tag{3}$$

$\overline{y} \text{ and } \overline{d}$ are the mean of $Y = \{y_1, y_2, ..., y_l, ..., y_N\}$ and $D = \{d_1, d_2, ..., d_l, ..., d_N\}$ vectors respectively.

But R is strongly affected by extreme values (Kemal & Ayen, 2008). To fill this gap, another quality measure is the normalized root mean square error (NRMSE) (equation 4). The value is often expressed as a percentage. A low *NRMSE* reflects a better fit.

$$NRMSE = \frac{\sqrt{MSE}}{d_{max} - d_{min}} \tag{4}$$

The input parameters used generating the maximum PGA of the three directions in the free-field are the M_{JMA} magnitude (Japanese Meteorological Agency magnitude), the focal depth D (km), the epicentral distance d (km), the thickness of the sedimentary layers Z_{800} (m) below the site down to a shear wave velocity equal to 800 m/s and the corresponding resonant frequency f_{800} (Hz) (Figure 2).
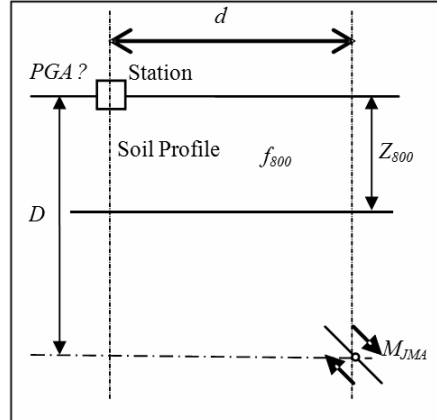

Figure 2. Site seismic parameters.

The accelerogram can be described as the convolution of the source effect and two filters, the path effect and the site effect. The source is describe by its magnitude which reflects the energy release during the earthquake. PGA is directly related to the earthquake magnitude: the larger the magnitude, the larger the PGA. The seismic waves attenuate while propagating through the crust, and the amplitude decrease is related to the source-to-site distance. This attenuation depends on the depth of the earthquake focus and on the epicentral source-to-site distance. PGA decreases with increasing distance from the source.

Moreover, site effects might influence PGA. In most seismic codes, site effects are taken into account by the introduction of the shear velocity at the site. In the Uniform Building Code, UBC97 (Klimis, 1998) average shear wave velocity down to thirty meters (V_{s30}) is considered. In some cases, a site classification based on V_{s30} is rather used. In both cases, only superficial properties of the soil are considered. However, a deeper geological structure such as sedimentary basins can have a strong influence on the seismic signal (Lussou, 2001).

In this work two site parameters Z_{800} and f_{800} are used which take into account the thickness of the sedimentary layers and the average shear wave velocity in this sedimentary layer. Z_{800} is the depth down to a velocity of 800 m/s. f_{800} is estimated from:

$$f_{800} = \frac{\sum_I^n h_I \Big/ \sum_I^n \left(h_I / V_{sI} \right)}{4 \times Z_{800}}$$ (5)

h_I represents the thickness of the Ith layer and V_{sI} is the shear velocity of the Ith layer.

SELECTED KIK-NET DATASET

The database used in this study includes 2176 accelerograms, from 238 earthquakes and 102 stations, freely available at: http://www.kik.bosai.go.jp (Figure 3).

The KiK-net network is composed of paired accelerometric sensors at the surface and at depth (between 80 and 1500 meters) (Pousse, 2005). The distribution of the data with respect to epicentral distance d, focal depth D, and magnitude M_{JMA}) is given in Figure 4.
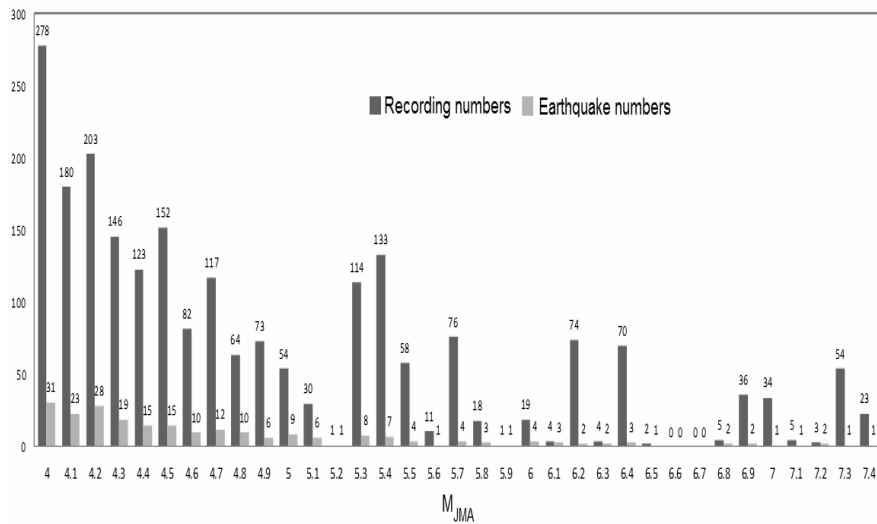

Figure 3. Distribution of number for ground motion used for PGA estimations.
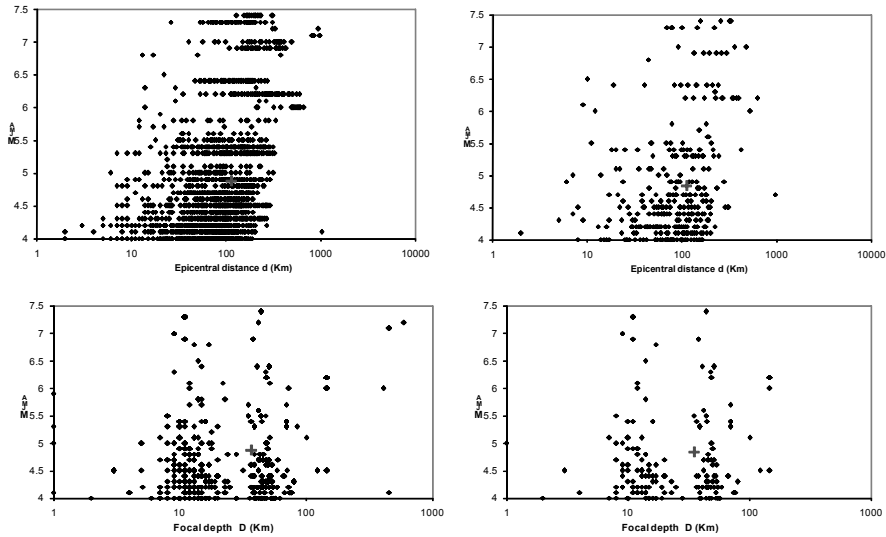
Figure 4. Magnitude-distance (top) and magnitude-focal depth (bottom) distributions for the training phase (left), the testing phase (right). "+" represents the average data.

The number of records used for the training of this neural model is 1850, and 326 of 2176 records are kept for the test phase. The "ViewWave" software version 1.53 (Kashima, 2007) was used to read the accelerograms, due to compatibility between this software and KiK-net records.

The KiK-net data also provide geotechnical characterization for each station. This information consists of lithology description, velocity profiles for both P and S waves. The Z_{800} is obtained directly from these profiles. Table 1 represents the recording stations used in this study with their site parameters Z_{800} and f_{800}.

ARTIFICIAL NEURAL NETWORK MODEL

The Artificial Neural Network Model of feed-forward back-propagation (FFBP) with a total connection is used to estimate the PGA from the source, path and site parameters (Figure 5). The NeuroSolutions software version 5.07 is used for this task (NeuroDimension, Inc).

The input parameters are chosen after several tests, in order to quantify the influence of each parameter and each group of parameters on the calculated PGAs. The PGA is expressed in natural logarithm (Ln) to reduce non-linearity in the model and it allows the analysis of normally distributed data.

TABLE 1

Recording Stations Used in this Study

| Site code	Z_{800} (m)	f_{800} (Hz)		Site code	Z_{800} (m)	f_{800} (Hz)		Site code	Z_{800} (m)	f_{800} (Hz)
EHMH01	10	8.25		KGWH01	34	2.04		SIGH03	39	2.61
EHMH02	16	4.54		KGWH02	56	1.09		SIGH04	36	3.36
EHMH03	12	11.42		KOCH01	28	2.28		SMNH01	22	4.32
EHMH04	200	0.70		KOCH02	8	3.95		SMNH02	25	4.59
EHMH05	30	3.02		KOCH03	10	11.03		SMNH03	34	3.36
EHMH06	12.5	9.09		KOCH04	4	25.00		SMNH04	11	2.88
EHMH07	20	3.51		KOCH05	6	15.42		SMNH05	14	7.50
FKOH01	13	5.83		KOCH06	8	6.25		SMNH06	30	2.40
FKOH02	25	2.39		NARH01	26	2.89		SMNH07	60	1.74
FKOH03	25	4.32		NARH02	12	4.71		TKSH01	16	4.82
FKOH04	35	3.91		NARH03	12	4.89		TKSH02	14	3.65
FKOH05	3	11.67		NARH04	22.75	5.29		TKSH03	20	3.52
HRSH01	28	3.42		NARH05	18	3.82		TTRH01	32	3.40
HRSH02	12	4.11		NARH06	13.75	3.85		TTRH02	100	1.31
HRSH03	20	4.63		NIGH11	185	0.71		TTRH03	74	1.11
HRSH04	16	4.38		NIGH12	110	1.58		WKYH01	10	5.10
HRSH05	56	2.14		OKYH01	44	1.53		WKYH02	16	3.51
HRSH06	51	2.73		OKYH02	8	12.91		WKYH03	16	5.74
HRSH07	52	2.40		OKYH03	20	2.74		WKYH04	4	53.38
HRSH08	12	11.41		OKYH04	10	3.77		WKYH05	16	5.59
HRSH09	14	5.99		OKYH05	10	8.41		WKYH06	5	14.50
HRSH10	42	1.82		OKYH06	24	5.21		WKYH07	27	2.70
HYGH01	74	1.39		OKYH07	6	21.25		WKYH08	25	3.33
HYGH02	14	6.80		OKYH08	12	10.00		WKYH09	76	1.68
HYGH03	8	6.02		OKYH09	21	4.71		WKYH10	18	4.36
HYGH04	22	3.61		OKYH10	8	7.81		YMGH02	20	3.58
HYGH05	13	5.56		OKYH11	20	5.13		YMGH03	24	4.72
HYGH06	32	2.96		OKYH12	12	7.92		YMGH04	12	7.38
HYGH07	14	5.55		OSKH01	550	0.23		YMGH05	24	3.80
HYGH08	24	2.51		OSKH02	600	0.21		YMGH07	20	3.31
HYGH09	52	2.25		OSKH03	24	3.50		YMGH08	16	3.31
HYGH10	82	0.96		OSKH04	16	5.39		YMGH09	28	2.59
HYGH11	50.5	1.51		SIGH01	14	6.25		YMGH10	18	5.50
HYGH12	13	8.38		SIGH02	6	10.83		YMGH11	16	7.95
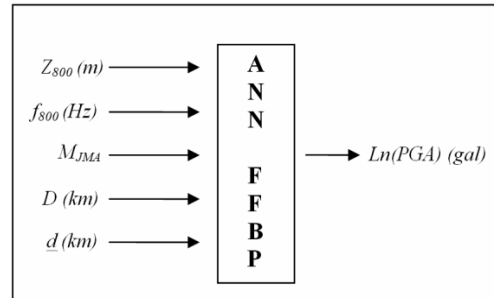
Figure 5. Neural network input parameters.

To build the neural network, the recommendations given by Seung and Sang (2002) were applied using a single hidden layer whose number of neurons is equal to six which is the sum of the input and output neurons. The maximum error (*ME*) tolerated by the neural network is obtained through the following relationship (Seung & Sang, 2002) :

$$M\hat{E} < \frac{1}{2}\left(minoutput^2 \times Nbr(neurones_{output})\right)$$ (6)

Where $minoutput$ represents the minimum value of the desired output, and $Nbr(neurones_{output})$ denotes the number of neurons in the output layer, (here 1).

In addition, the number of epochs is set to 1000 and the updating of weights is done by batch (all the inputs in the training set are applied to the network before the weights are updated). Moreover, the activation function for neurons in the input and hidden layers is Tanh-sigmoid and linear for neurons in the output layers (which is the best combination after the tests performed as will be shown later). The tests results are listed in Tables 2, 3 and 4. In these lists, the *MSE* and *R* for training and testing phases are calculated.

TABLE 2

Influence of Each Parameter on the Model Reliability

Type of parameters	parameters	MSE_{train}	R_{train}	MSE_{test}	R_{test}
Seismic Parameters	(M_{JMA})	0.089	0.36	0.091	0.28
	(D)	0.099	0.11	0.111	0.10
	(d)	0.075	0.51	0.076	0.48
Site parameters	(f_{800})	0.101	0.037	0.106	0.035
	(Z_{800})	0.098	0.16	0.110	0.13
	$(f_{800})+(Z_{800})$	0.097	0.21	0.098	0.18

Table 2 lists the *MSE* and *R* for different tests using different combinations of inputs. From the values of *MSE* and *R*, one can notice that each parameter affects differently the overall results given by the neural network. The best values of *R* are 0.51 and 0.48 associated with small values of *MSE* equal to 0.075 and 0.076, for the training and testing

phases respectively. These values correspond to the epicentral distance d which is the primary parameter affecting the PGA. On the other hand, hypocentral depth, resonant frequency and sedimentary layer thickness have only a small impact if a single input parameter is considered.

TABLE 3

Influence of Combinations of Parameters on the Model Reliability

Type of Parameters	Parameters	MSE_{train}	R_{train}	MSE_{test}	R_{test}
Seismic Parameters	d + D	0.078	0.52	0.083	0.46
	d + M	0.039	0.78	0.048	0.74
	d + D + M	0.038	0.79	0.042	0.77
Seismic Parameters + Site Parameters	d +D +M +f_{800}	0.0342	0.81	0.041	0.78
	d +D +M + Z_{800}	0.033	0.82	0.036	0.80
	d +D +M +f_{800} + Z_{800}	0.0203	0.85	0.0205	0.84

Table 3 shows the results using different combinations of input parameters. The best values of R are 0.85 for training and 0.84 for testing using all the parameters associated with small MSE values. One concludes that all considered input parameters do influence the value of PGA. In the following, all five parameters, namely $d + D + M + f_{800} + Z_{800}$, will be used as inputs to the neural model.

The nature of the activation function has a great influence on the model. One may conduct some tests on the neural network to choose the appropriate function for this model (Table 4). Five activation functions are tested.

TABLE 4

Influence of Different Activation Functions

Activation function of hidden layer	Activation function of the output layer	MSE train	R train	MSE test	R test
Log-sigmoid	Log-sigmoid	0.062	0.74	0.071	0.72
Log-sigmoid	Linear log-Sigmoid	0.064	0.75	0.061	0.69
Log-sigmoid	Linear	0.035	0.80	0.039	0.79
Tanh-sigmoid	Tanh-sigmoid	0.028	0.85	0.031	0.84
Tanh-sigmoid	Linear Tanh-sigmoid	0.032	0.83	0.034	0.82
Tanh-sigmoid	Linear	0.020	0.85	0.021	0.84

A speed reading of Table 4 shows that the best combination of activation functions is the tangent hyperbolic function for the hidden layer and linear for the output layer.

RESULTS AND DISCUSSION

To see if the neural model predicts well the PGA with other data, the comparison between the recorded PGAs and the ones estimated by the neural model is represented in Figure 6. This test was made with data that are not used in the training phase. The test was done with 15% of the total database (326 recordings) (Figure 5), and the PGAs range between 0.10 and 544.57 gal. This comparison reveals an *MSE* equal to 0.020 for the training and 0.021 for the test.
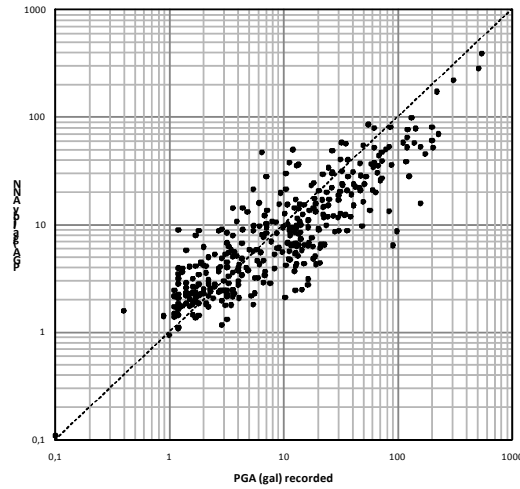

Figure 6. Recorded versus predicted PGAs.

To quantify the ability of this model to predict PGA, it was compared with two other GMPEs derived for the Japanese region. The first was established by Takahashi *et al.* (2000) and is supposed to be applicable in Japan:

$$log_{10}(PGA) = 0.446\,M_W - 0.0035\,d - Log_{10}(d + 0.012.10^{0.446\,M_w}) + 0.00665(D - 20) + s \quad (7)$$

Where PGA is in gal (cm/s²), *d* and *D* are the epicentral distance and focal depth (in km). "s" is the coefficient which depends on the soil type (rock, firm, soft or very soft soil) and M_w is the moment magnitude (Figure 7).

The second attenuation relationship chosen to compare with the neural model is the one obtained by (Ambraseys & Douglas, 2003). The general form of the equation for predicting the PGA is:

$$PGA_{10}(PGA) = -0.659 + 0.202M_s - 0.0238 + 0.025_A + 0.029S_s \quad (8)$$

Where PGA is in m/s², *d* is the epicentral distance (km), M_s is the surface wave magnitude and both S_A and S_s are coefficients related to the site effect.

To compare the two GMPEs with this neural model, one must take into account the difference in the magnitude scales that are used by each model. Figure 7 shows the relationship between different types of magnitudes and the moment magnitude M_w. The saturation of all the magnitude scale is clear from this figure starting at magnitude around 6 for M_L and around 7.5 for M_s. However, in the magnitude range of 4.5-7.5 of this data set, the values of M_w, M_s and M_{JMA} are similar, and consequently no conversion will be performed.
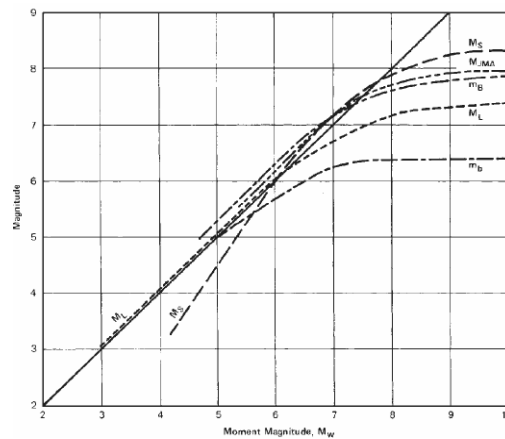

Figure 7. Relationship between M_w and the different types of magnitudes (Amr & Luigi, 2008).

Among the 326 earthquakes used in the test phase, only 55 are used for the comparison which have focal depth lower than 19 km which is the limit of validity of Ambraseys's GMPE.

Table 6 shows the performance of each of the three models. The coefficients of determination R^2, show that the PGAs estimated by the neural method are in better agreement with the data (R^2=0.94) compared with the PGAs estimated from the two GMPEs (R^2=0.82 and R^2=0.76). Among the three models used, the neural model NMRSE value of 0.11 is the smallest (Table 5).

TABLE 5

Statistical Parameters of Measure

Model chosen	R^2	NRMSE (%)
(Ambraseys & Douglas, 2003)	0.76	0.25
(Takahashi *et al.*, 2000)	0.82	0.17
Neural model	0.94	0.11

This result is confirmed also by observing the 55 PGAs chosen for this comparison (Figure 8). The PGA, which is significantly closer to the middle line y = x is the one estimated by the neural model.
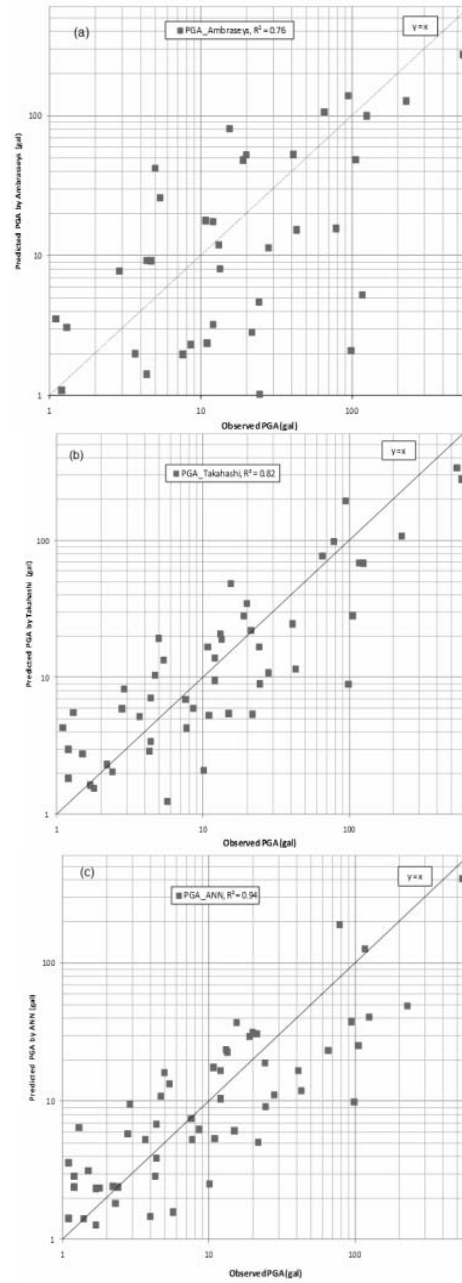
Figure 8. Comparison of observed and predicted PGA using (a) the Ambraseys GMPE, (b) the Takahashi model and (c) the neural model.

CONCLUSION

In this study, a new method for deriving Ground-Motion Prediction Equations for PGA was proposed based on the feed-forward neural network with a conjugate gradient back-propagation rule for the training. Data from the dense KiK-net network are analyzed.

No functional form is defined *a priori* and input parameters are the magnitude JMA (M_{JMA}), the epicentral distaince (D), the focal depth (d), and site conditions represented by the depth Z_{800} and the frequency f_{800}

The tests performed on the input parameters show that magnitude and distance are first order parameters influencing PGA. Focal depth and site parameters have a small influence compared to the distance and magnitude. It is interesting to note that focal depth and site parameters have an equivalent influence on PGA. The test also shows that a combination of all five parameters gives the best results.

The type of activation function plays an important role. This function allows the introduction of nonlinearity in the network and therefore allows a better modeling of complex phenomena. Another test was conducted to make the choice of the activation function that should be used in the neural model. The result shows that the configuration with a hyperbolic tangent function for the hidden layer and a linear one for the output layer gives the best results.

The validation of this neural network model is achieved by comparing results obtained by the neural model and those obtained by two classical GMPEs for crustal earthquakes: one based on Japanese data (Takahashi *et al*., 2000) and one based en Euro-Mediteranean data (Ambraseys & Douglas, 2003). Although the three models use different magnitude scales, they are equivalent in the magnitude range of the data and no conversion is performed.

The results of the comparison show that among the two classical GMPEs, the one derived from Japanese data performs better than the other one. This raises the question of regional dependence of ground-motion which is a highly debated issue. The results also show that the neural network model performs considerably better than the other two. One reason could be the use of focal depth as input parameter which is not, or only partially, taken into account in classical GMPE. It is believed that the model developed in this paper is a good alternative to classical GMPEs and could be used in seismic hazard assessment studies.

In the future, the f_{800} could be replaced by the fundamental frequency at the site f_0, as determined from H/V measument, which better represents the fundamental frequency of the site than the f_{800} used in the present study. Z_{800} might also be replaced by V_{s30} which is now available at many accelerometric stations. Doing so, the ANN model could be tested using many different databases around the world. Different kind of neural networks can also be used such as the Network Radial Basis Functions (RBF) and the hybrid approach Neuro-Fuzzy.

REFERENCES

Alves, E.I. 2006. Earthquake forecasting using neural networks: results and future work. *Nonlinear Dynamics,* 44: 341–349.

Ambraseys, N.N. and Douglas, J. 2003. Near-field horizontal and vertical earthquake ground motions. *Soil Dynamics and Earthquake Engineering*, 23(1): 1 – 18.

Amr, S.E. and Luigi, D.S. 2008. *Fundamentals of earthquake engineering.* A John Wiley & Sons, Ltd, Publication United Kingdom.

Baziar, M.H. and Ghorbani, A. 2005. Evaluation of lateral spreading using artificial neural networks. *Soil Dynamics and Earthquake Engineering,* 25: 1–9.

Ben-yu, L., Liao-Yuan, Y., Mei-Ling, X. and Sheng, M. 2006. Peak ground velocity evaluation by artificial neural network for West America region. *The 13th International Conference on Neural Information Processing ICONIP 2006*, part II, LNCS 4233, pp. 942-951.

Chu-Chieh, J.L and Jamshid, G. 2001. Generating multiple spectrum compatible accelerograms using stochastic neural networks. *Earthquake Engng. Struct. Dyn.*, 30: 1021–1042.

Coulibaly, P., Anctil, F. and Borée, B. 1999. Prévision hydrologique par réseaux de neurones artificiels : état de l'art. *CNRC Canada Eng.*, 26: 293-304.

Demuth, H., Beale, M. and Hagan, M. 2009. *Neural Network Toolbox™ 6.* User's Guide. Copyright 1992–2009 by The MathWorks, Inc.

Derras, B., Bekkouche, A. and Zendagui, D. 2010. Neuronal approach and the use of kik-net network to generate response spectrum on the surface. *Jordan Journal of Civil Engineering*, 4: 12-21.

Douglas, J. 2003. Earthquake ground motion estimation using strong-motion records: a review of equations for the estimation of peak ground acceleration and response spectral ordinates. *Earth-Science Reviews*, 61(1-2): 43–104.

Irshad, A., El Naggar ,H. and Khan, A.N. 2008. Neural networks based attenuation of strong motion peaks in Europe. *Journal of Earthquake Engineering*, 12: 663-680.

Ghaboussi, J. and Lin, C.J. 1998. New method of generating spectrum compatible accelerograms using neural networks, *Earthquake Engineering & Structural Dynamics*, 27: 377-396.

Giacinto, G., Paolucci, R., Roli, F. 1997. Application of neural networks and statistical pattern recognition algorithms to earthquake risk evaluation. *Pattern Recognition Letters,*18(11-13): 1353-1362.

Goh, A.T.C. 1994. Seismic liquefaction potential assessed by neural networks. *ASCE Journal of Geotechnical Engineering*, 120 : 1467-1480.

Kashima, T. 2007. *ViewWave Help.*Version 1.53, IISEE, BRI.

Kemal, G. and Ayen, G. 2008. Peak ground acceleration prediction by artificial neural networks for Northwestern Turkey. *Hindawi Publishing Corporation Mathematical Problems in Engineering*, vol. 2008, article ID 919420, 20 pages doi:10.1155/2008/919420.

Klimis, N.S., Margaris, B.N., Koliopoulos, P.K. 1998. Response spectra estimation according to the EC8 and NEHRP soil classification provisions: a comparison study based on Hellenic data. *11th European Conference on Earthquake Engineering*, Balkema, Rotterdam, ISBN 90 5410 982 3.

Lussou, P., Bard, P.Y. and Cotton, F. 2001. Site design regulation codes: contribution of K-NET DATA to site effect evaluation. *Journal of Earthquake*, 5(1): 13-33.

Lussou, P. 2001. *Calcul du mouvement sismique associé à un séisme de référence pour un site donné avec prise en compte de l'effet de site. Méthode empirique linéaire et modélisation de l'effet de site non-linéaire*. Thèse de doctorat, Université de Grenoble, 2001.

Moré, J.J. 1978. *The Levenberg-Marquardt algorithm: implementation and theory* (lecture notes in mathematics), 630, G.A. Watson, ed., Springer-Verlag, Berlin-Heidelberg-New York, pp.105-116.

NeuroDimension, Inc. *NeuroSolutions Getting Started Manual Version 5*. www.nd.com.

Paolucci, R., Colli, P. and Giacinto, G. 2000. Assessment of seismic site effect in 2-D alluvial valleys using neural networks. *Eartquake Spectra*, 16(3): 661-680.

Pousse,.G. 2005. *Analyse des données accélérometriques de K-NET et KIK-NET : implications pour la prédiction du mouvement sismique -accélérogrammes et spectres de réponse et la prise en compte des effets de site nonlinéaire*. Thèse de Doctorat, octobre 2005, IRSN-2006-65.

Seung, C.L. and Sang, W.H. 2002. Neural-network-based models for generating artificial earthquakes and response spectra. *Computers and Structures,* 80: 1627–1638.

Takahashi, T., Kobayashi, S., Fukushima, Y., Zhao, J.X., Nakamura, H. and Somerville, P.G. 2000. A spectral attenuation model for Japan using strong - motion data base. *Proceedings of the 6th International Conference on Seismic Zonation: Managing Earthquake Risk in the 21st Century*, Earthquake Engineering Research Institute, Oakland, CA, USA.

Tienfuan, K. and Ting, S.B. 2005. Neural network estimation of ground peak acceleration at stations along Taiwan high-speed rail system. *Engineering Applications of Artificial Intelligence,* 18: 857–866.

Vincenzo, B., Matteo, C., Sebastiano, D., Antonino, G., Francesco, C.M. and Francesco, P. 2006. *Radial basis function neural networks to foresee aftershocks in seismic sequences related to large earthquakes*. ICONIP., Part II, LNCS4233, pp. 909–916. Springer-Verlag Berlin Heidelberg.

Yu, H.H. and Jenq-Neng, H. 2002. *Handbook of neural network signal processing*. CRC press, pp. 408.